

# Performance Comparison of PPM-TH, PAM-TH, and PAM-DS UWB Rake Receivers with Channel Estimators via Correlation Mask

Shing TenqChen<sup>1&†</sup>, Ying-Haw Shu<sup>1</sup>, Ming-Chang Sun<sup>1</sup>, Wu-Shiung Feng<sup>††</sup> and Chao-Hao Lee<sup>†</sup>

<sup>1&†</sup>The author is with the department of Electrical Engineering, National Taiwan University (NTU-EE) & ChungHwa Telecom Labs (CHTTL), Taoyuan, Taiwan 326.

<sup>††</sup>The author is with the department of Electronics Engineering, Chang Gung University,

<sup>†</sup>The author is with CHTTL, Taiwan.

**Abstract:** - In this paper, the performance comparison of PPM-TH, PAM-TH, and PAM-DS UWB for a single user link are analyzed for different data rates using the proposed UWB channel model from IEEE 802.15.3a. The Rake receivers with a pulse-matched filter via correlation mask are numerically evaluated with channel estimator algorithm. DS-UWB and TH-UWB with antipodal modulation perform basically the same. However, since TH-UWB is more difficult to synthesize, the conclusion is that DS-UWB is more suitable for high-speed indoor links. System based on TH show that, in general, it is less robustness against acquisition errors compared with that of DS-UWB.

**Key-Words:** - PPM-TH UWB, PAM-DS UWB, DS-UWB, FH-SS, IEEE 802.15.3a, Rake receivers.

## 1 Introduction

UWB is defined by the Federal Commission (FCC) as any wireless transmission scheme that occupies a fractional bandwidth  $W/f_c \geq 20\%$  where  $W$  is the transmission bandwidth and  $f_c$  is the band center frequency [1]-[5]. In the near future, there will be a strong demand for low cost, high-speed, wireless links for short range (<10 m) communications. Such links should support digital video transmission without the need of cable. One of the promising techniques is UWB. It is characterized by the transmission of very short pulses, which occupy large frequency bandwidth. This paper compares three single-band impulse radio systems, namely pulse-position modulation time-hopping (PPM-TH) spread-spectrum impulse radio, pulse-amplitude modulation (PAM-TH), and direct-sequence spread-spectrum impulse radio (PAM-DS) UWB. Both DS-UWB and TH-UWB are spread-spectrum systems. In DS-UWB, the pulses are transmitted conditionally using a pseudorandom sequence for the spreading of information bits, and in TH-UWB, a pseudorandom sequence defines the time when the pulses are transmitted.

The classical binary PAM can be presented using two antipodal Gaussian pulses. The square wave represents the random code, which affects the polarity of the individual pulses, which make up the DS waveform. Recent proposals in the USA, and in the IEEE 802.15.TG3a Working Group, refer to a multiband (MB) alternative to DS-UWB in which the overall available bandwidth is divided into sub-bands of at least 500 MHz. Frequency-Hopping spread spectrum (FH-SS) might also be a viable path. TH-UWB and DS-UWB may adopt in principle either PPM or PAM for data modulation. Thus, this paper describes the comparison of performance for PPM-TH, PAM-DS UWB wireless communications to propagate over a multi-path-affected UWB radio channel to compare their system throughputs.

## 2 UWB Data modulation

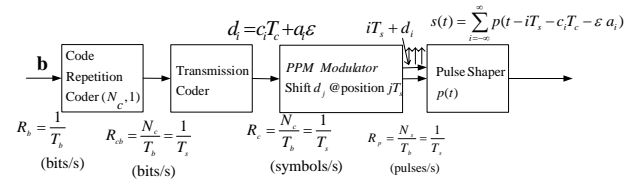


Fig. 1(a) Transmission scheme for a PPM-TH UWB.

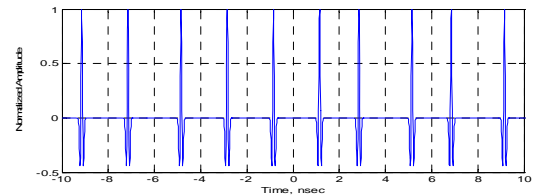


Fig.1(b) Time window of a transmitted data bit for PPM-TH-UWB spreading in the case of Pow=-30; fc=50e9; numbits=2; Ts=3e-9; Ns=5; Tc=1e-9; Np=5; Tm=0.5e-9; tau=0.25e-9; and dPPM=0.5e-9.

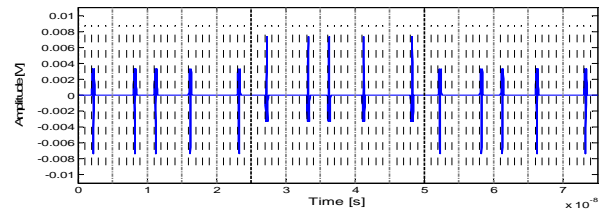


Fig.1(c) Time window of a transmitted data bit for PAM-TH UWB transmitter (Pow=-30, fc=50e9, numbits=3, Ts= 5e-9, Ns=5, Tc=1e-9, Nh=5, Np=5, Tm=0.5e-9, tau=0.25e-9, THcode=[2 3 1 1 3]).

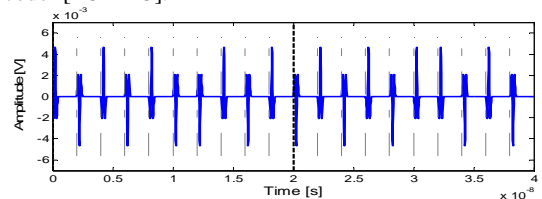


Fig.1(d) Time window of a transmitted data bit for PAM-DS UWB transmitter in the case of Pow=-30, fc=50e9, numbits=2, Ts=2e-9, Ns=10, Np=10, Tm=0.5e-9, tau = 0.25e-9, and DS code.

In TH-UWB combined with binary PPM (binary PPM-TH-UWB or 2PPM-TH-UWB), the UWB signal can be schematized to be generated as shown in Fig. 1(a) and the output waveforms are shown in Figure 1(b)-1(d). Given the channel model of Eq. (1)

$$h^{(m)}(t) = \sum_{l=0}^{\infty} \alpha_l \delta(t - \tau_l)$$

$$\sum_{i=1}^{N_t} \sum_{m=0}^{\infty} \sum_{n=0}^{\infty} \alpha^{(m)} e^{j\theta_{m,n}} \delta(t - iT_m - \tau_{m,n}^{(i)}) \quad (1)$$

where  $T_m + \tau_{m,n}$  ( $\tau_{m,0} = 0$ ) denotes the arrival time of the  $n$ th multiple component of the  $m$ th cluster,  $\theta_{m,n}$  are independent uniform random variables over  $[0, 2\pi)$ , and  $\alpha_{m,n}$  are independent Rayleigh random variables with power  $E\{\alpha_{m,n}^2\} = E\{\alpha_{0,0}^2\} e^{-T_m/\Gamma} e^{-\tau_{m,n}/\gamma}$ , where  $\Gamma > \gamma$ .

The number of clusters and multipath components may theoretically extend over infinite time. The binary PPM-TH, PAM-TH and PAM-DS UWB signal transmitted by  $m$ th user for  $N_s$  pulses on each bit. We will accordingly define those three different schemes. The second block called a transmission coder applies an integer-valued code  $\mathbf{c} = (\dots, c_0, c_1, \dots, c_i, c_{i+1}, \dots)$  to the binary sequence  $\mathbf{a} = (\dots, a_0, a_1, \dots, a_i, a_{i+1}, \dots)$  and generates a new sequence  $\mathbf{d}$ . The generic element of the sequence  $\mathbf{d}$  is expressed as follows  $d_i = c_i T_c + a_i \varepsilon$ , where  $T_c$  and  $\varepsilon$  are constant terms that satisfy the condition  $c_i T_c + \varepsilon < T_s$  for all  $c_i$ . The coded real-valued sequence  $\mathbf{d}$  entered a third system, the PPM modulator, which generates a sequence of unit pulses at a rate of  $R_p = N_s / T_b = 1 / T_s$  pulses/s. These pulses are located at times  $iT_s + d_i$ , and are shifted in time from nominal positions  $iT_s$  by  $d_i$ . Note that the code  $\mathbf{c}$  introduces a TH shift on the generated signal, and it is for this reason that it is indicated as TH code. Note that the shift introduced by the PPM modulator is usually much smaller than the shift introduced by the TH code,  $c_i T_c$ . To allow for multi-user access (MA) to the UWB channel, time hopping (TH) was introduced earlier in [10]. With TH, each pulse is positioned within each frame duration  $T_f$ , according to a user-specific TH sequence  $c_u^{TH}(n)$ . Specifically, dividing each frame into  $N_c$  chips for each duration  $T_c$ , the  $u$ th user's TH code  $c_u^{TH}(n) \in [0, N_c - 1]$  corresponds to a time shift of  $c_u^{TH}(n) T_c$  during the  $n$ th frame. Consequently, the  $u$ th user's transmitted signal  $v_u(t)$  is expressed as following

$$v_u(t) = \sqrt{E_u} \sum_{n=0}^{\infty} a_u(\lfloor n/N_f \rfloor) \cdot p(t - nT_f - c_u^{TH}(n)T_c - b_u(\lfloor n/N_f \rfloor)\Delta), \quad (2)$$

where  $E_u$  is the  $u$ th user's energy per pulse at the transmitter end. With  $s_u(k) \in [0, M - 1]$  denoting the  $M$ -ary information symbol transmitted by the  $u$ th user during the  $k$ th symbol duration. Eq. (2) preserves several modulation schemes. When  $a_u(k) = 1$  and  $b_u(k) = s_u(k)$  Eq. (2) describes  $M$ -ray PPM-TH. When  $a_u(k) = 2s_u(k) + 1 - M$ , and  $b_u(k) = 0$  Eq. (2) denotes  $M$ -ary PAM. With binary symbols, and when  $a_u(k) = 2s_u(k) - 1$ , and  $b_u(k) = 0$  corresponds to BPSK, and  $a_u(k) = s_u(k)$  defines the OOK [2], [8]. With TH codes, MA is achieved by altering the pulse position from frame to frame, according to the sequence  $c_u^{TH}(n)$ . In binary PPM, the delay can be chosen to

minimize the correlation  $\int p(t)p(t-\Delta)dt$  [8].  $p(t)$  denotes the transmitted pulseform that has a maximum amplitude of one, a duration  $T_c$  and is transmitted with a repetition period  $T_s$ . MA can also be enabled by modifying the pulse amplitude from to frame. Eq. (2) allows for many other choices of alternative spreading codes, direct-sequence (DS-UWB) [4], or base-band single-carrier/multicarrier (SC/MC)-UWB [2], just to name a few. The generated signal is described as follows

$$v_u(t) = \sqrt{E_u} \cdot \sum_{n=0}^{\infty} a_u(\lfloor n/N_f \rfloor) c_u(n) \cdot p(t - nT_f - c_u^{TH}(n)T_c - b_u(\lfloor n/N_f \rfloor)\Delta), \quad (3)$$

where  $c_u(n)$  is the user-specific amplitude code during the  $n$ th frame. Let us define the symbol level transmitted waveform for user  $u$  when there is no spreading code involved as follows

(a) PPM-TH-UWB

$$p_{T,u}(t) := \sum_{n=0}^{N_f-1} p(t - nT_f - c_u^{TH}(n)T_c - a_i \varepsilon), \quad (4)$$

where an additional time-shift  $a_i \varepsilon$  whose value depends on whether  $a_i$  is +1 or -1. The general signals of PAM-TH UWB and PAM-DS UWB are described as

(b) PAM-TH-UWB

$$p_{T,u}(t) := \sum_{n=0}^{N_f-1} p(t - nT_f - c_u^{TH}(n)T_c), \quad (5)$$

(c) PAM-DS-UWB

$$p_{T,u}(t) := \sum_{n=0}^{N_f-1} p(t - nT_f), \quad (6)$$

respectively. Along the lines of [5], it can be shown that

the power spectral density (PSD) of Eq. (2) for  $v_u(t)$  is

$$\Phi_{vv}(f) = \frac{E_u}{T_s} |P_{T,u}(f)|^2 \sum_{n=-\infty}^{\infty} \phi_{aa}^{(n)} \phi_{bb}^{(n)}(f) e^{-j2\pi f n T_s}, \quad (7)$$

where

$$\phi_{aa}^{(n)} := E\{a_u(k)a_u(k+n)\}, \quad (8)$$

$$\phi_{bb}^{(n)}(f) := E\{e^{-j2\pi f(b_u(k)-b_u(k+n)\Delta)}\}, \quad (9)$$

and

$$P_{T,u}(f) := \mathcal{F}\{p_{T,u}(t)\} \quad (10)$$

respectively.

### 3 IEEE UWB Channel Model

The IEEE 802.15.3a Channel-Modeling sub-committee finally converged on a model based on the cluster approach proposed by Turin and others in 1972 [3] and further formalized by Saleh and Valenzuela (S-V model) in 1987 [4]. The S-V model is based on the observation that usually multipath contributions generated by the same pulse arrive at the receiver grounded into clusters. According to Foerster, a discrete time multipath channel impulse can be expressed as follows:

$$h_i(t) = X_i \sum_{l=1}^{L_c} \sum_{k=0}^{K_{LC}} \alpha_{k,l}^i \delta(t - T_l^i - \tau_{k,l}^i) \quad (11)$$

where  $\alpha_{k,l}^i$  represents the multipath gain coefficients,  $T_l^i$  the delays of the  $l$ -th cluster,  $\tau_{k,l}^i$  gives the delays for the  $k$ th multipath component relative to  $l$ -th cluster the arrival time.  $X_i$  represents the shadowing effect of log-normal distributed and  $i$  refer to the  $i$ th realization.  $L_c$  is the number of observed clusters,  $K_{LC}$  is the number of multi-path contribution of the  $n$ -th cluster,  $T_n$  is the time of arrival of the  $n$ -th cluster, and  $\Lambda$  is the cluster arrival rate;  $\lambda$  is the ray arrival rate. The time of arrival of clusters is modeled as a Poisson arrival process with rate  $\Lambda$ :

$$p(T_l | T_{l-1}) = \Lambda e^{-\Lambda(T_l - T_{l-1})}, \quad l > 0 \quad (12)$$

where  $T_l$  and  $T_{l-1}$  are the times of arrival of the  $l$ -th and  $(l-1)$ -th clusters, respectively. We set  $T_l=0$  for the first cluster. With each cluster, subsequent multipath contributions also arrive according to Poisson process with rate  $\lambda$ :

$$p(\tau_{k,l} | \tau_{(k-1),l}) = \lambda e^{-\lambda(\tau_{k,l} - \tau_{(k-1),l})}, \quad k > 0. \quad (13)$$

where  $\tau_{k,l}$  and  $\tau_{(k-1),l}$  are the time of arrival of the  $k$ -th and  $(k-1)$ -th contributions within clusters  $l$ . The channel coefficient  $\alpha_{k,l}$  defined by [4] can be defined as follows:

$$\alpha_{k,l} = p_{k,l} \xi_l \beta_{k,l} \quad \text{and} \quad (14)$$

$$20 \log_{10}(\xi_l \beta_{k,l}) \propto N(\mu_{k,l}, \sigma_1^2 + \sigma_2^2), \quad \text{or} \quad (15)$$

$$|\xi_l \beta_{k,l}| = 10^{(\mu_{k,l} + n_1 + n_2)/20}, \quad (16)$$

where  $n_1 \propto N(0, \sigma_1^2)$  and  $n_2 \propto N(0, \sigma_2^2)$  are independent and correspond to the fading on each cluster and ray, respectively, and

$$E\left[|\xi_l \beta_{k,l}|^2\right] = \Omega_0 e^{-T_l/\Gamma} e^{-\tau_{k,l}/\gamma}, \quad (17)$$

where  $\Omega_0$  is the mean energy of the first path of the first cluster,  $T_l$  is the excess delay of bin  $l$  and  $p_{k,l}$  is a discrete equiprobable  $\pm 1$  to account for signal inversion due to reflection. The  $\mu_{k,l}$  is given by [4]

$$\mu_{k,l} = \frac{10 \ln(\Omega_0) - 10 T_l / \Gamma - 10 \tau_{k,l} / \gamma - (\sigma_1^2 + \sigma_2^2) \ln 10}{\ln(10)}. \quad (18)$$

The variables in the above equations represent the fading associated with the  $l$ -th cluster,  $\xi_l$ , and the fading associated with  $k$ th ray of the  $l$ -th cluster,  $\beta_{k,l}$ . The shadowing term is characterized by [4]

$$20 \log_{10}(X_i) \propto N(0, \sigma_x^2). \quad (19)$$

In addition to cluster and ray decay factor,  $\Lambda$  and  $\lambda$  are the model inputs cluster and ray decay factors  $\Gamma$  and  $\gamma$ , respectively. The standard deviation terms in dB for cluster lognormal fading, ray lognormal fading and lognormal shadowing term for total multipath realization  $\sigma_1, \sigma_2$  and  $\sigma_x$ , respectively.

Four different channel implementations are suggested, which are based on the average distance between transmitter and receiver, and whether a line-of sight (LOS) channel is present or not. SV-1: LOS model for 0-4m, SV-2: Non-LOS (NLOS) channel for 0-4m, SV-3: NLOS for 4-10m model, and SV-4: NLOS for an extreme NLOS multipath channel condition. The four channel models and their parameters are listed in Table 2.1 [4]. The damped sine waves and their Fourier transform is shown in Fig. 2.

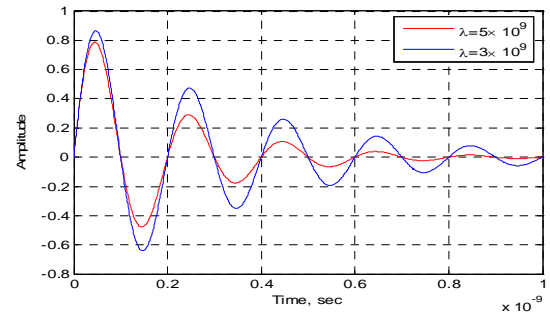


Fig.2 Damped sine waves and their Fourier transforms.

Table 3.1 the main parameters are presented in the IEEE 802.15.3 proposal and the Simulink model is shown in Fig.3. The output waveform of SV-1 and SV-2 are shown in Figure 4 and (5) for LOS case.

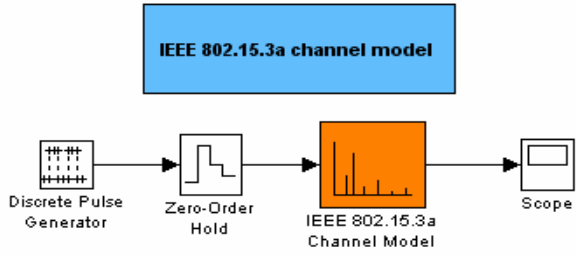
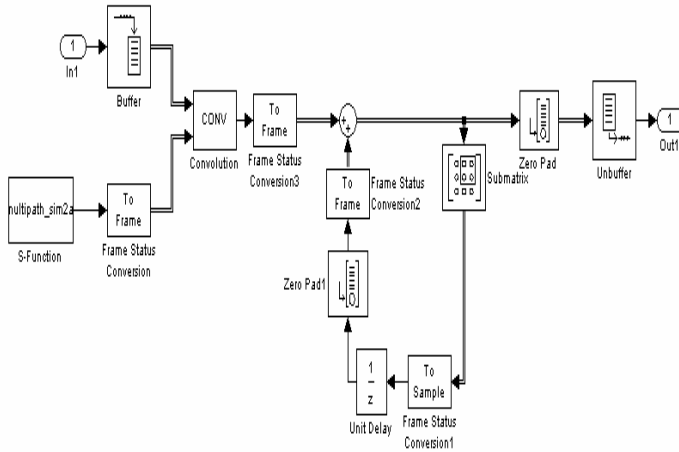


Fig.3 IEEE802.15.3Simulink Model and its inside block.



Target channel characteristics	SV-1	SV-2	SV-3	SV-4
Model parameters				
$\Lambda$ (1/nsec) (LAMDA)	0.0233	0.4	0.0667	0.0667
$\lambda$ (1/nsec) (lamda)	2.5	0.5	2.1	2.1
$\Gamma$ (GAMMA)	7.1	5.5	14.00	24.00
$\gamma$ (gamma)	4.3	6.7	7.9	12
$\sigma_1$ (dB)	3.3941	3.3941	3.3941	3.3941
$\sigma_2$ (dB)	3.3941	3.3941	3.3941	3.3941
$\sigma_3$ (dB)	3	3	3	3

Table 3.1 Main parameters of IEEE 802.15.3a.

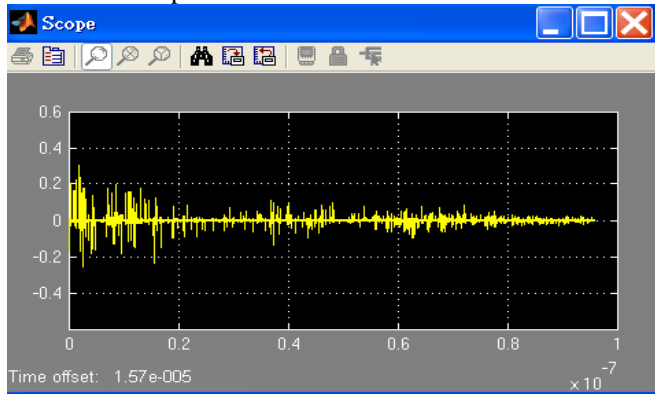


Fig. 4 The output waveform of LOS channel model.

### III. Coherent RAKE Receiver Algorithm

In this paper, we investigate coherent, selective Rake- $N$

receiver. First, the output from a pulse-matched filter is sampled at a given rate which is equal to symbol, chip, or a fraction of the chip rate. If the signals from Rake fingers are uncorrelated and have the same noise power, the algorithm achieves the theoretical performance of the maximum-ratio combining (MRC), which maximizes the signal-to-noise ratio.

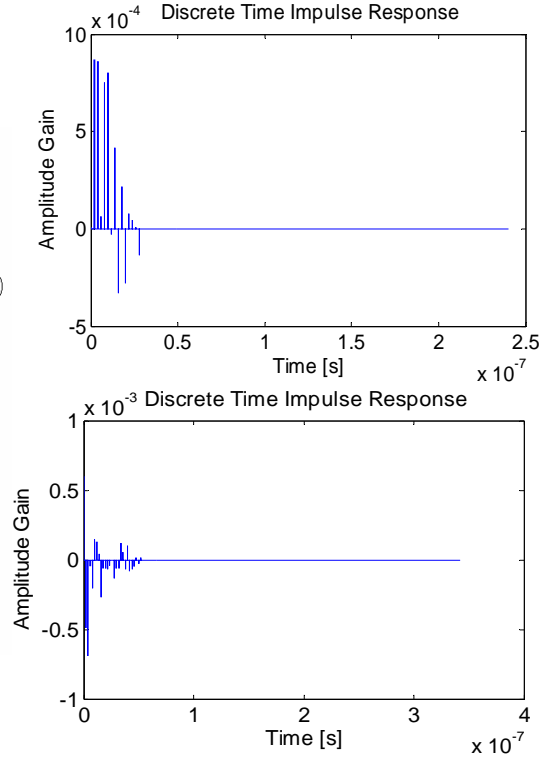


Fig. 5 (a) SV-1: LOS (b) SV-2: NLOS model from top.

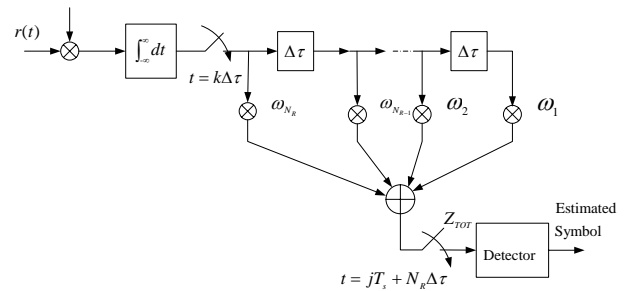


Fig. 6. RAKE Receiver for discrete-time Channel.

Given the discrete-time channel model of (11) shown in Fig. 6 and the presence of thermal noise at the channel output, the receiver is given by the sum of all signals originating from the  $N_u$  transmitters, and can be written as follows:

$$r(t) = X \sqrt{E_{TX}} \sum_{n=1}^{N_u} \sum_{k=1}^{K(n)} \alpha_{nk} a_j p_0(t - jT_s - \phi_j - \tau_{nk}) + n(t) \quad (20)$$

where  $X$  is the log-normal distributed amplitude gain of the channel,  $E_{TX}$  is the transmitted energy per pulse,  $N_u$  is the number of clusters observed at destination,  $K(n)$  is the number of multi-path contributions associated with the  $n$ -th cluster,  $\alpha_{nk}$  is the channel coefficient of the  $k$ -th path within the  $n$ -th cluster,  $a_j$  is the amplitude of the  $j$ -th

transmitted pulse ( $a_j=1$  in the case of PPM),  $\tau_{nk}$  is the delay of the  $k$ -th path within the  $n$ -th cluster and  $E_{RX}^{(n)} = E_{TX}^{(n)} (\alpha^{(n)})^2$ . The energy contained in the channel coefficients  $\alpha_{nk}$  is normalized to unity for each realization of the channel impulse response, that is:  $\sum_{n=1}^{N_c} \sum_{k=1}^{K(n)} |\alpha_{nk}|^2 = 1$ . The system schematic model for the asynchronous system under investigation in Figure 7.

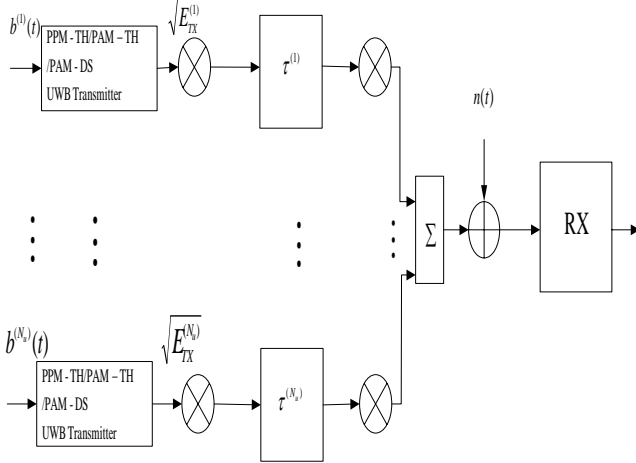


Fig.7 Multiuser PPM-TH/PAM-TH/PAM-DS UWB Model

Performance of the RAKE receiver for propagations over a multi-path channel can be evaluated by the first assuming a specific model for the channel impulse response, and by evaluating the probability of error on the symbol  $Pr_e$  as a function of the  $E_{RX}/N_0$  ration for the different diversity methods. This analysis is performed in general under the assumption of perfect knowledge of the coefficients of the channel impulse response, or perfect channel estimation. The first strategy, called selective RAKE (SRake), consists of selecting the  $L_B$  best components among the  $L_{TOT}$  available at the receiver input. The number of branches of the RAKE is reduced, but the receiver still must keep track of all the multi-path components to perform the selection. A second and simpler solution, called partial RAKE (PRake), combines the first arriving  $L_p$  paths without operating any selection among all available multi-path components.

Given the symmetry of the model, we can focus the analysis on the active link. Suppose the reference receiver is listening to the first transmitter (TX1). Under the hypothesis of perfect synchronization between the TX1 and reference receiver, the time delay  $\tau^{(1)}$  is known by the receiver, and one can assume  $\tau^{(1)} = 0$  given that only relative delays and phases are relevant. The received signal can thus be rewritten as follows:

$$r(t) = r_u(t) + r_{mui}(t) + n(t), \quad (21)$$

where  $r_u(t)$  and  $r_{mui}(t)$  are useful signal and MUI contributions at the receiver input. With soft decision at the receiver, the analysis focuses on a bit time interval of duration  $T_b$ . Given again the symmetry of the system, the analysis can be focused on the interval  $[0, T_b]$ . The

$r_u(t)$  and  $r_{mui}(t)$  contributions can be written as follows:

$$r_u(t) = \sum_{i=0}^{N_s-1} \sqrt{E_{RX}^{(1)}} p_0(t - iT_s - c_i^{(1)}T_c - a_i^{(1)}\varepsilon) \quad \forall t \in [0, T_b], \quad (22)$$

$$r_{mui}(t) = \sum_{n=2}^{N_c} \sum_{i=0}^{N_s-1} \sqrt{E_{RX}^{(n)}} p_0(t - iT_s - c_i^{(n)}T_c - a_i^{(n)}\varepsilon - \tau^{(n)}) \quad \forall t \in [0, T_b]. \quad (23)$$

The average symbol error rate coincides with the average bit error rate  $Pr_b$  since modulation is binary and corresponds to the probability of misdetecting a reference bit  $b$  transmitted by TX1. To perform the function of the receiver for PPM-TH-UWB signals, there exist three steps. Step one defines the receiver setting, which is dependent on what kind of the selection of soft or hard decision detection is made. Step two implements both correlators and detector, and step three generates the statistics. To measure receiver performance, the estimated binary stream at the output of the detector is compared with the original binary stream at the output of the stream produced by the transmitter. For each stream of estimated bits,  $Pr_b$  is determined by dividing the number of wrong bits by the total number of transmitted bits.

The reference bit  $b$  is defined as the bit received in the time interval  $[0, T_b]$ . The soft decision correlation receiver output, as described in [1], can be expressed as follows:

$$Z = \int_{mt_b}^{(m+1)t_b} r(t)m(t)dt \quad (24)$$

where  $m(t)$  is the correlation receiver mask and is defined as follows:

$$m(t) = \sum_{i=0}^{N_s-1} v(t - iT_s - c_i^{(1)}T_s) \quad (25)$$

$$\text{with } v(t) = p_0(t) - p_0(t - \varepsilon). \quad (26)$$

The decision rule based on the maximum likelihood (ML) criterion for both orthogonal and optimum binary PPM implies the comparison of  $Z$  against a threshold that is zero in the case of Eq. (24) and (26). We know that this detector is optimum if noise is additive and Gaussian, and coincides with the maximum a posteriori (MAP) if all received signals are equally probable, as in the present case. The ML decision rule can be thus expressed as follows:

$$\text{ML receiver decision rule : if } \begin{cases} Z > 0 \Rightarrow \hat{b} = 0 \\ Z < 0 \Rightarrow \hat{b} = 1, \end{cases} \quad (27)$$

where  $\hat{b}$  indicates the estimated bit. The decision rule based on the Maximum Likelihood (ML) criterion for both orthogonal and optimum binary PPM implies the comparison of  $Z$  against a threshold that is zero in the case of Eqs. (24)-(26). By combining Eq. (22) and (24), one can write:

$$Z = Z_u + Z_{mui} + Z_n \quad (28)$$

where  $Z_u$ ,  $Z_{mui}$ , and  $Z_n$  indicate that a useful signal, MUI noise, and thermal noise at the receiver output.  $Z_{mui}$  can be removed at the receiver if all codes were orthogonal at the receiver under perfect synchronization of all users in the

system. The first term  $Z_u$  is deterministic when reference bit  $b$  is fixed. According to the decision rule of Eqs. (20), and given equally probable source symbols, the probability of bit errors  $Pr_b$  is given by

$$\begin{aligned} Pr_b &= \frac{1}{2} \Pr(\hat{b} = 1|b = 0) + \frac{1}{2} \Pr(\hat{b} = 0|b = 1) \\ &= \Pr(Z < 0|b = 0). \end{aligned} \quad (29)$$

According to the standard Gaussian approximation (SGA),  $Z_{mui}$  and  $Z_n$  are a zero-mean Gaussian random process characterized by variance  $\sigma_{mui}^2$  and  $\sigma_n^2$ , respectively. Under the SGA hypothesis, the relation between  $Pr_b$  and  $SNR_{spec}$  can be extended by

$$Pr_b = \frac{1}{2} \operatorname{erfc} \left( \sqrt{\frac{SNR_{spec}}{2}} \right) \quad (30)$$

which accounted for thermal noise and incorporated with the current case of MUI. The useful signal contribution is the bit energy  $E_b$ , therefore, one can write:

$$SNR_{spec} = \frac{E_b}{\sigma_n^2 + \sigma_{mui}^2}. \quad (31)$$

By isolating thermal and MUI contributions, Eq. (29) can be rewritten as follows:

$$SNR_{ref} = ((SNR_n)^{-1} + (SIR)^{-1})^{-1} = \left( \left( \frac{E_b}{\sigma_n^2} \right)^{-1} + \left( \frac{E_b}{\sigma_{mui}^2} \right)^{-1} \right)^{-1} \quad (32)$$

where  $SNR_n$  and  $SIR$  are the signal to thermal and MUI ratios, respectively. The variance of thermal noise at the binary PPM receiver output  $\sigma_n^2$  is expressed as follows:

$$\sigma_n^2 = N_s N_0 (1 - R_0(\varepsilon)) \quad (33)$$

which leads to the following expression for  $SNR_n$ :

$$SNR_n = \frac{N_s E_{RX}^{(1)}}{N_0} (1 - R_0(\varepsilon)) = \frac{E_b}{N_0} (1 - R_0(\varepsilon)). \quad (34)$$

As above discussed, Eq. (34) shows that  $SNR_n$  is maximum when  $R_0(\varepsilon)$  is minimum, and can be maximized by selecting an optimal  $\varepsilon$  value. This procedure leads to optimal binary PPM. Let us characterize MUI. Since the system is asynchronous, we consider the interference events for all cases where the receiver detects an alien pulse. Figure 8 shows the effect of the presence of an interference noise at the output of the receiver.

## 4 Conclusion

UWB systems may be primarily divided into impulse radio (IR) systems and multiband systems. Multiband systems offer the advantage of potentially efficient utilization of spectrum. However, IR systems have the significant advantage of simplicity, and so are potentially lower costs. The performance of the synchronous and asynchronous systems for the TH system is very similar. This is because each user has a different pulse transmit

instant associated with their PR sequence, so the pulses are offset even if the time hopping frames are aligned. The performances of the TH and DS asynchronous systems are very similar. This is to be expected in an AWGN channel with low duty cycle pulses. As expected, SRake outperforms PRake since it achieves higher SNR at the output of the combiner. The gap in performance, however, decreases when the best paths are located at the beginning of the channel impulse response as it happens, when considering LOS scenarios.

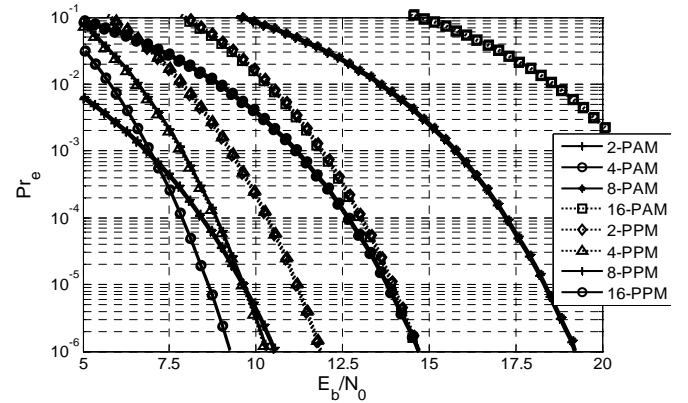


Fig.8 Probability of error  $Pr_e$  vs.  $E_b/N_0$  for binary PPM & PAM.

## REFERENCES

- [1] M. Z. Win and R. A. Scholtz. Ultra-wide bandwidth time-hopping spread spectrum impulse radio for wireless-access communication. *IEEE Transactions on Communications*, 48(4):679-691, April 2000.
- [2] Ian Opperman, Matti Hämäläinen, Jari Linatti, UWB Theory and Applications, *John Wiley & Sons, Ltd*, England 2004.
- [3] G.L. Turin, F.D. Clapp, T.L. Johnson, S.B. Fine, and D. Lavry, "A Statistical Model of Urban Multipath Propagation," *IEEE Transactions Vehicular Technology*, Vol. 21, pp.1-9, 1972.
- [4] J. Foerster, M. Pendergrass, and A. F. Molisch, "A channel model for ultra-wideband indoor communications", *Proc. of the 6<sup>th</sup> International Symposium on Wireless Personal Multimedia Communications*, Yokosuka, Japan, pp. 116-120, 2003.
- [5] J. Proakis, *Digital Communication*, McGraw-Hill, Inc, 3<sup>rd</sup> Edition, Singapore, pp. 751-777, 1995
- [6] P. Withington, R. Reinhardt and R. Stanley, (1999) Preliminary results from ultra-wideband (impulse) scanning receivers', *Proc. Of the IEEE Military Communications Conference (MILCOM '99)*, Atlantic City, NJ USA, pp. 1186-1190.
- [7] M. Hämäläinen, V. Hovinen, R. Tesi, J. Linatti, M. Lavtva-aho, "On the UWB System co-existence with GSM900, UMTS/WCDMA and GPS", *IEEE Journal on Selected Areas in Communications*, 20, No. 9, p. 1712-1921, 2002.
- [8] R. A. Scholtz, "Multiple access with time-hopping impulse modulation," in *Proc. MILCOM Conf.*, Boston, MA1993, pp. 447-450.